^1H and ^{15}N NMR Assignments of PsaE, a Photosystem I Subunit from the Cyanobacterium *Synechococcus* sp. Strain PCC 7002†

Christopher J. Falzone,*,‡ Yung-Hsiang Kao,‡ Jindong Zhao,§ Kristen L. MacLaughlin,‡ Donald A. Bryant,*,§ and Juliette T. J. Lecomte*,‡

Department of Chemistry, Department of Biochemistry and Molecular Biology, and Center for Biomolecular Structure and Function, The Pennsylvania State University, University Park, Pennsylvania 16802

Received January 5, 1994; Revised Manuscript Received March 9, 1994⊕

ABSTRACT: PsaE is a highly conserved, water-soluble protein of the photosystem I reaction center complexes of cyanobacteria, algae, and green plants. Along with the PsaC and PsaD proteins, the PsaE protein binds to the stromal surface of photosystem I and is required for cyclic electron transport in *Synechococcus* sp. strain PCC 7002 [Yu, L., Zhao, J., Mühlenhoff, U., Bryant, D. A., & Golbeck, J. H. (1993) *Plant Physiol. 103,* 171–180]. The *psaE* gene from this cyanobacterium encodes a mature protein of 69 amino acid residues and has recently been overexpressed in *Escherichia coli* [Zhao, J., Snyder, W. B., Mühlenhoff, U., Rhiel, E., Warren, P. V., Golbeck, J. H., & Bryant, D. A. (1993) *Mol. Microbiol. 9,* 183–194]. By using both unlabeled and uniformly ^{15}N-labeled protein in a series of two- and three-dimensional NMR experiments, complete ^1H and ^{15}N amide resonance assignments were made. The major secondary structural element of PsaE is a five-stranded antiparallel β-sheet. The five strands extend as follows: βA, residues 7–10; βB, residues 21–26; βC, residues 36–39; βD, residues 57–60; and βE, residues 65–68. The topology is represented by (+1, +1, +1, −4*x*); it brings the first and last strands, and consequently the N- and C-termini, together. The protein has an extensive hydrophobic core organized around a conserved phenylalanine residue (Phe-40); another of its distinctive features is a segment extending from residue 42 to residue 56 devoid of dipolar contacts with the β-sheet. The $pK_{1/2}$ of the sole histidine residue (His-63) was determined to be 5.4.

The PsaE[1] protein is a subunit of the photosystem I (PS I) reaction center complex that is found in all oxygen-evolving photosynthetic organisms, including cyanobacteria, eukaryotic algae, and higher plants. PS I functions as a membrane-bound, photooxidoreductase and catalyzes the light-driven transfer of an electron from reduced plastocyanin (or cytochrome c_6) to oxidized ferredoxin [or flavodoxin; for reviews, see Bryant (1992), Chitnis and Nelson (1991), Golbeck (1992, 1994), and Golbeck and Bryant (1991)]. The cyanobacterial PS I complex is made up of 11 polypeptide subunits, about 100 chlorophyll *a* molecules, 10–15 β-carotenes, 2 vitamin K_1 molecules, and 3 [4Fe-4S] centers denoted F_X, F_A, and F_B. The PsaE subunit is associated with the stromal side of the PS I complex (P700–F_X) core protein (Li et al., 1991a; Parrett et al., 1990). PsaC, PsaD, and PsaE from the cyanobacterium *Synechococcus* sp. PCC 7002 have been overproduced in *Escherichia coli* and used in reconstitution studies *in vitro* with PS I core protein (Li et al., 1991b; Zhao et al., 1993; W. M. Schluchter, J. Zhao, L. Yu, J. H. Golbeck, and D. A. Bryant, unpublished results).

Cyanobacterial PsaE proteins are basic polypeptides (p*I*s 8–10) composed of 69–75 amino acid residues. Although the cyanobacterial proteins are significantly smaller than their nuclear encoded homologues from higher plants (91–101 amino acids), all PsaE proteins, regardless of source, are about 60% identical in their C-terminal domains (Bryant, 1992). No significant sequence homology to other proteins has been found in database searches. Cross-linking studies with PS I complexes from higher plants suggest that PsaE interacts with ferredoxin:$NADP^+$ oxidoreductase (Andersen et al., 1992). However, the functional role of PsaE in cyanobacterial PS I complexes that do not bind ferredoxin:$NADP^+$ oxidoreductase (Schluchter & Bryant, 1992) was not clearly defined until recently. No phenotypic differences were originally observed for interposon mutants in which the *psaE* genes were insertionally inactivated (Bryant et al., 1990; Chitnis et al., 1989). More detailed studies revealed that a *psaE* mutant strain of *Synechococcus* sp. PCC 7002 could not grow photoheterotropically and exhibited impaired growth at low light intensity or low (atmospheric) carbon dioxide levels (Zhao et al., 1993). These results suggested that the PsaE subunit might play a role in cyclic electron transport, and this suggestion has been confirmed by electron transport studies in intact cyanobacterial cells (Yu et al., 1993). *In vitro* studies have also suggested that PsaE may promote an interaction between the PsaC, which binds the terminal-accepting Fe-S centers F_A and F_B, and soluble ferredoxin and thereby enhance photoreduction rates of this soluble electron acceptor (Rousseau et al., 1993; Sonoike et al., 1993; Weber & Strotmann, 1993).

† This work was supported in part by National Science Foundation Grant MCB-920576 (D.A.B.) and by National Institutes of Health Grant DK-43101 (J.T.J.L.).

* Address correspondence to D.A.B. regarding the biochemistry and molecular biology of photosystem I and to C.J.F. or J.T.J.L. regarding NMR matters.

‡ Department of Chemistry.

§ Department of Biochemistry and Molecular Biology.

⊕ Abstract published in *Advance ACS Abstracts,* April 15, 1994.

[1] Abbreviations: 1D, one dimensional; 2D, two dimensional; 3D, three dimensional; DIPSI, decoupling in the presence of scalar interactions; GARP, globally optimized alternating phase rectangular pulse; HSQC, heteronuclear single-quantum coherence; NOE, nuclear Overhauser effect; NOESY, nuclear Overhauser enhancement spectroscopy; PS, photosystem; PsaE, photosystem I accessory protein E; 2QF-COSY, double-quantum-filtered correlation spectroscopy; 3QF-COSY, triple-quantum-filtered correlation spectroscopy; 2Q, double quantum; TOCSY, totally correlated spectroscopy; TPPI, time-proportional phase incrementation; WALTZ, wide-band alternating phase low-power technique for zero residue splitting.

0006-2960/94/0433-6043$04.50/0

From X-ray crystallographic studies of the trimeric PS I complex of the thermophilic cyanobacterium *Synechococcus* sp., a low-resolution (6-Å) structural model has recently been determined (Krauss et al., 1993). The main protein structural elements visible at this resolution are numerous transmembrane α-helices, although several extramembrane α-helices are also observed. The three [4Fe-4S] centers are clearly distinguishable on the stromal side of the complex, but the PsaC, PsaD, and PsaE proteins are only visible as an unstructured lump extending about 35 Å from the stromal membrane surface [see also Böttcher et al. (1992) and Kruip et al. (1993)]. In order to provide additional structural details of the acceptor-side proteins of PS I, an NMR study of the PsaE protein of *Synechococcus* sp. PCC 7002 was initiated. Conditions for the overproduction of this protein as inclusion bodies, its renaturation, and its rebinding to the PS I complex or thylakoids of the *psaE* mutant of the same organism were recently reported (Zhao et al., 1993). The initial steps in the structural analysis by NMR methods were to establish the conditions under which the protein could be studied, to assign its ^1H and ^{15}N spectrum, and to describe its secondary structure and global fold. In this paper, these initial results are presented as they provide the basis for the structural determination described in the accompanying paper (Falzone et al., 1994).

MATERIALS AND METHODS

Protein Overproduction and Purification. Overexpression of the *Synechococcus* sp. strain PCC 7002 *psaE* gene in *E. coli* strain BL21 (DE3) cells in rich medium and inclusion body isolation were performed as described previously (Zhao et al., 1993). Purification was carried out as described below for the ^{15}N-labeled protein. To obtain ^{15}N-labeled protein, cells harboring plasmid pET-3d(*psaE*) (Zhao et al., 1993) were grown in M9 minimal medium (Maniatis et al., 1982) containing 1 g L^{-1} [^{15}N]ammonium chloride (Aldrich, Milwaukee, WI) and 50 μg mL^{-1} ampicillin. The M9 minimal medium was supplemented with 1.0 mL of P1 trace metal solution (Stevens et al., 1973), since this was found to increase the growth rate of cells approximately 2-fold and the final cell yield approximately 4-fold. A 10-mL overnight culture of cells grown at 37 °C was inoculated into 500 mL of M9 medium and incubated with shaking for 5 h before IPTG was added to a final concentration of 0.5 mM to induce the expression of the *psaE* gene. The culture was incubated with shaking for an additional 5–7 h. Cells were harvested by centrifugation at 3600*g* and washed twice with TS buffer (20 mM Tris-HCl, 20 mM NaCl, pH 8). The pelleted cells were stored at −80 °C until used for inclusion body purification.

Inclusion bodies were resuspended in a minimal volume of TS to which 10 M urea was added to a final concentration of 6.8 M. Dithiothreitol was also added to a final concentration of 2 mM from a 1 M stock solution. The solution was incubated at room temperature for 30 min and was then centrifuged at 106000*g* for 45 min. The supernatant containing solubilized PsaE was loaded onto a 2 × 25 cm gel filtration column (Ultrogel AcA-54 from LKB), and renatured PsaE was eluted with TS buffer containing 2 mM dithiothreitol, 5% glycerol, and 0.5 mM EDTA. Fractions containing monomeric PsaE were pooled and stored at 4 °C. Prior to NMR experiments, the protein was exhaustively dialyzed against phosphate buffer and concentrated by ultrafiltration over a YM3 membrane (Amicon, Beverly, MA) to a concentration of approximately 15–20 mg mL^{-1} PsaE. All preparations of PsaE used in these studies were tested for their ability to rebind to thylakoids isolated from a *psaE* mutant strain of *Synechococcus* sp. strain PCC 7002 (Zhao et al., 1993). The protein in all cases rebound and could subsequently be isolated as a stoichiometric component of the PS I complex after detergent solubilization of the thylakoid membranes.

Sample Preparation. For H_2O spectra, a solution of purified PsaE was concentrated to 2 mM by ultrafiltration as described above. ^2H_2O was added to bring the concentration of ^2H_2O to ca. 5% of the total volume. For ^2H_2O spectra, the sample was lyophilized once and dissolved in ^2H_2O. Sample concentrations were 1–2 mM and were obtained by UV absorbance at 280 nm (ϵ_{280} = 13 200 mM^{-1} cm^{-1}). The volume of the protein solutions was 0.45 mL contained in 5-mm OD NMR tubes.

NMR Spectroscopy. Spectra were collected at 298 K and pH 5.8 in both H_2O and ^2H_2O and referenced to the H_2O or $^2H^1HO$ resonance at 4.76 ppm. Two-dimensional data were also obtained at pH 3.7. NMR data were acquired with a Bruker AM-500 spectrometer. Standard pulse sequences were applied: 2QF-COSY (Rance et al., 1983), 3QF-COSY (Braunschweiler et al., 1983; Rance & Wright, 1986), 2Q (Braunschweiler et al., 1983; Rance & Wright, 1986), TOCSY (Braunschweiler & Ernst, 1983; Rance, 1987), and NOESY (Bodenhausen et al., 1984; Kumar et al., 1980). TOCSY and NOESY experiments were sine-modulated (Otting et al., 1986) with pulse-length compensation (Bax et al., 1991) and Hahn-echo observation (Rance & Byrd, 1983). TOCSY spectra were collected using DIPSI-2 for spin-locking (Shaka et al., 1988) with a mixing time of 42 or 47 ms. NOESY spectra were collected with mixing times of 70, 120, and 150 ms. A jump–return (Plateau & Guéron, 1982) 150-ms NOESY spectrum was also acquired on the H_2O sample; the parameters for this spectrum were identical to those of the NOESY spectrum recorded with the echo read pulse. TPPI (Drobny et al., 1979; Marion & Wüthrich, 1983) was used for quadrature detection in the indirectly acquired dimension for all proton data.

For the 2QF-COSY, 3QF-COSY, and 2Q spectra, the spectral width in the F_2 dimension was 6024 Hz over 2048 complex points. For NOESY and TOCSY experiments, the spectral width in the F_2 dimension was extended to 12 500 Hz, and 4096 complex points were acquired to improve the baseline. Only the central 6250 Hz of the transformed F_2 dimension was kept in the data matrix. The spectral width in the F_1 dimension was 6024 Hz for 2QF- and 3QF-COSY spectra, and between 512 and 600 t_1 increments were acquired whereas the NOESY and TOCSY experiments were collected over a spectral width of 6250 Hz in F_1 using 490–512 t_1 increments. The 2Q spectra were acquired with 512–800 t_1 increments using a spectral width of 12 500 Hz in the F_1 dimension. All two-dimensional proton data were zero-filled in the indirect dimension to give a final matrix of 2048 × 2048 real points. Data were processed using the program FTNMR by Dennis Hare or FELIX from Biosym Technologies running on an Iris 4D/240 GTX Silicon Graphics and an Indigo XZ4000 workstation, respectively. A sine-bell window with a $\pi/8$ shift was applied in the F_1 and F_2 dimensions to most data sets except to NOESY data, which were subjected to a Gaussian window (Gaussian parameter of 0.2 and a line broadening of −2 Hz) for the purpose of volume integration.

^1H-^{15}N HSQC data sets (Bodenhausen & Ruben, 1980) were collected with a spectral width of 12 500 Hz in the ^1H (F_2) dimension using 4096 complex points and 2000 or 1700 Hz in the ^{15}N (F_1) dimension. A total of 128–360 t_1 increments were used in the final data matrix, which consisted of 512 (^{15}N) × 1024 (^1H) real data points and contained the central 6250 Hz in F_2. Either 16 or 32 transients were acquired for each t_1 point with GARP-1 (Shaka et al., 1985) or WALTZ-

16 (Shaka et al., 1983) decoupling being applied during acquisition. To identify the backbone amide hydrogens that exchange slowly with the solvent, the ^{15}N-labeled protein was dissolved in ^2H_2O and ^1H–^{15}N HSQC spectra were acquired every 30 min for 3 h and then every hour for 15 h. The decoupling sequence was generated either by explicitly writing the pulses in the pulse program or by using a GARP box from Tschudin Associates (Kensington, MD) to generate the required pulse train (Kay et al., 1990).

The 3D ^{15}N NOESY–HSQC and TOCSY–HSQC data sets were acquired with mixing times of 120 and 40 ms, respectively. The spectral widths in F_3 (^1H), F_2 (^{15}N), and F_1 (^1H) dimensions were 4000, 1700, and 7000 Hz, respectively and the corresponding carriers were placed at 8.00, 116, and 4.76 ppm. From 29 to 32 complex data points were collected for the 3D NOESY data sets. The TOCSY data were acquired with a timer accessory (Tschudin Associates) (Kay et al., 1990) which greatly reduces the total acquisition time by requiring fewer pulse trains to reach steady state and less time to compile the pulse program. TPPI was used for quadrature detection in the F_1 dimension whereas TPPI-States (Marion et al., 1989) was used in the F_2 (^{15}N) dimension. After zero-filling, final data matrices for the 3D data sets were $1024 \times 64 \times 512$ real data points. The ^{15}N spectra were indirectly referenced to [^{15}N]aniline at 56 ppm.

A set of eight J-modulated ^1H–^{15}N HSQC experiments were performed with mixing times ranging from 52 to 116 ms for measuring the $^3J_{\alpha H-NH}$ coupling constant (Billeter et al., 1992; Neri et al., 1990). The spectral widths were 12 500 and 2000 Hz for F_2 and F_1 dimensions, respectively. The ^1H carrier was placed on the water resonance (4.76 ppm), and the ^{15}N carrier was placed at 116 ppm. The intensity of the signals was measured and plotted as a function of the mixing time. Nonlinear least-squares fitting to a single exponential relaxation decay modulated by a cosinusoidal function of J as in eq 1 yielded the necessary J values. In this equation I is the

$$I = I_0 \cos(\pi^3 J_{\alpha H-NH} \tau) \exp(-\tau/T) \quad (1)$$

intensity of the cross peak of interest, I_0 is the amplitude at $\tau = 0$, T is a relaxation parameter, and τ is the mixing time. A Karplus equation (De Marco et al., 1978) translated these measurements into estimates of the backbone dihedral angle ϕ.

A 2D H_NNH_{AB} COSY experiment (Chary et al., 1991) was used to estimate the ^{15}N–H_β coupling constants needed for stereospecific assignments. The small negative ^3J ^{15}N–H_β values (De Marco et al., 1978) provide one of the criteria for making stereospecific assignments of β-methylene protons and for distinguishing between unique conformations about χ_1 or averaged rotamer populations (Clore & Gronenborn, 1989). The spectral widths in F_2 (^1H) and F_1 (^{15}N) were 12 500 and 2000 Hz, respectively; 2048 complex points were acquired in the directly observed dimension, and 112 t_1 values were measured with 512 transients per t_1 value; the ^1H carrier was set at 4.76 ppm and the ^{15}N carrier placed at 116 ppm. TPPI was used for quadrature detection in the F_1 domain.

pH Titration. The $pK_{1/2}$ of the single imidazole group (His-63) was determined in a 1D NMR pH titration carried out by adding aliquots of NaO^2H or ^2HCl to an unbuffered ^2H_2O solution of the protein. The pH ranged from 9.3 to 2.1. The chemical shift versus pH data were analyzed by nonlinear least-squares fitting to the Henderson–Hasselbalch equation with an adjustable Hill coefficient. Acid denaturation was monitored by measuring the integrated intensity of the simulated His-63 $C^\epsilon H$ resonance in the native and denatured forms. The fraction of native form versus pH data were also fit to the Henderson–Hasselbalch equation.

RESULTS AND DISCUSSION

The PsaE protein dissolved in H_2O at pH 5.8 and room temperature yields a 1D ^1H NMR spectrum characteristic of a folded polypeptide (Bundi & Wüthrich, 1979). In particular, amide signals resonate down to 9.6 ppm and methyl signals up to –0.34 ppm. The spectral dispersion reflects that the protein does indeed refold during application to the sizing column used for the purification. The 1D spectrum is reproducibly obtained with different protein preparations and with lyophilized protein. When the freeze-dried powder is dissolved in ^2H_2O, several amide resonances are seen to exchange slowly with solvent deuterons at pH 5.8. Since the purified material can be reconstituted with either the isolated PS complex or thylakoid membranes of a *psaE* mutant strain of *Synechococcus* sp. PCC 7002 (Zhao et al., 1993), a structural study of isolated PsaE appeared both feasible and of functional interest.

NMR Assignments. In order to assign the ^1H NMR spectrum of PsaE, a standard set of 2D experiments was performed. Identification of most of the side-chain resonances was possible through correlated spectroscopy (2Q, 2QF-COSY, 3QF-COSY, and TOCSY experiments). Figure 1A illustrates the quality of the data with a section of the aliphatic region obtained in a 2QF-COSY spectrum. Several of the valine and leucine isopropyl groups are directly recognized in this region of the plot; however, there is a high degree of degeneracy that renders identification of all methyl groups difficult. The 3QF-COSY spectrum (Figure 1B) was most convenient to distinguish the $C^\delta H_3$ group of isoleucines among the other signals.

Once the identification of the side-chain resonances could be initiated, a backbone-based strategy (Wüthrich, 1986) was employed to assign sequentially the ^1H resonances of PsaE. PsaE contains a single tryptophan residue (Trp-17) that gives rise to a typical pattern in the correlated spectra of the aromatic region. From the resonance identification of Trp-17, including its backbone protons through NOEs, it was possible to progress to the neighboring tyrosine residues (the protein sequence is contained in Figure 5). There were several other strategic starting points in the primary structure: *e.g.*, the sequences Ile-32–Ile-33–Tyr-34 and Val-36–Ile-37–Val-38.

Figure 2 shows the sequential assignment of residues 1–9 in the fingerprint region of a 70-ms NOESY spectrum. The interresidue $\alpha N(i, i+1)$ NOEs are connected and indicated by their sequential residue numbers; the intraresidue $N\alpha(i, i)$ NOEs, generally weaker, are the intervening cross peaks on the trace. Strong $\alpha N(i, i+1)$ NOEs are observed along this stretch of amino acids except for Gly-5 to Ser-6. These two residues give rise to an $NN(i, i+1)$ NOE in the lower section of the spectrum (not shown) indicating a turn of the polypeptide chain. Approximately 70% of the ^1H spectrum could be readily elucidated by applying these homonuclear methods.

An attempt to resolve additional resonances by changing the pH to a more acidic value was not entirely successful, and further confirmation for the ambiguous 30% of the signals required experiments more elaborate than homonuclear 2D ones. The problem stems mostly from chemical shift degeneracies of several amide protons: four resonate at 8.66 ppm, three at 8.68 ppm, two at 8.70 ppm, two at 7.87 ppm, and two at 7.88 ppm. These overlaps hinder the interpretation of the NOESY data, and in order to complete the ^1H assignments, it was necessary to study the ^{15}N-labeled protein. Figure 3

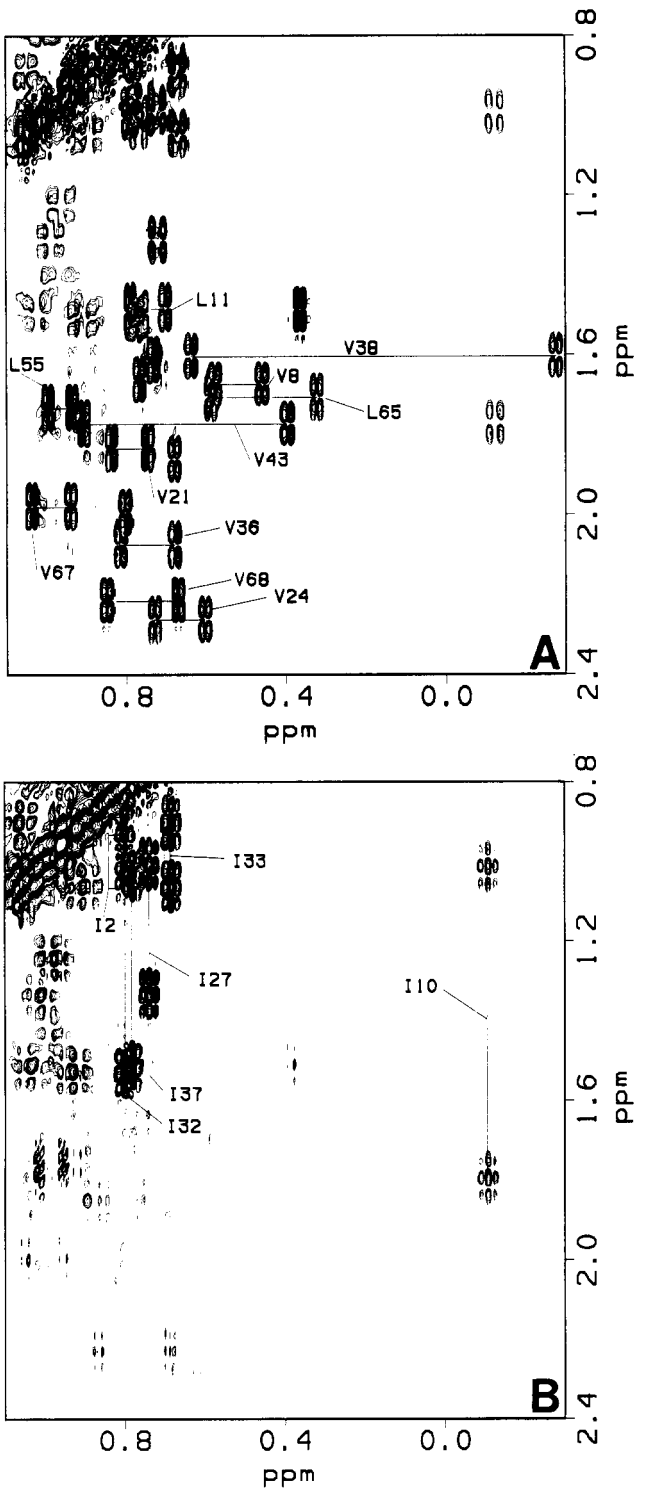

FIGURE 1: Partial aliphatic region from COSY spectra of PsaE at 298 K and pH 5.8 in ^2H_2O. (A) 2QF-COSY data show the isopropyl portion of Val and Leu spin systems. (B) 3QF-COSY data emphasize the $C^\delta H_3$ resonances of Ile spin systems. Assignments are described in the text and are listed in Table 1. All spectral data presented in this paper were collected at the same pH and temperature and at 11.7 T.

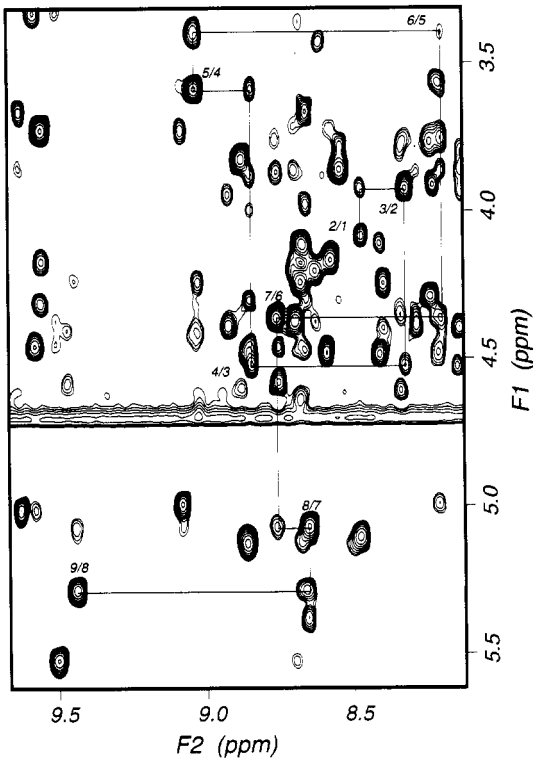

FIGURE 2: Fingerprint region of a 70-ms NOESY spectrum showing the sequential NOEs for residues 1–9. These $\alpha N(i, i+1)$ NOEs, in the absence of $NN(i, i+1)$ contacts, are indicative of an extended conformation. A backbone-based assignment (Wüthrich, 1986) strategy was applied to these resonances. Residues 4–6 have $NN(i, i+1)$ NOEs (not shown) that may indicate a turn.

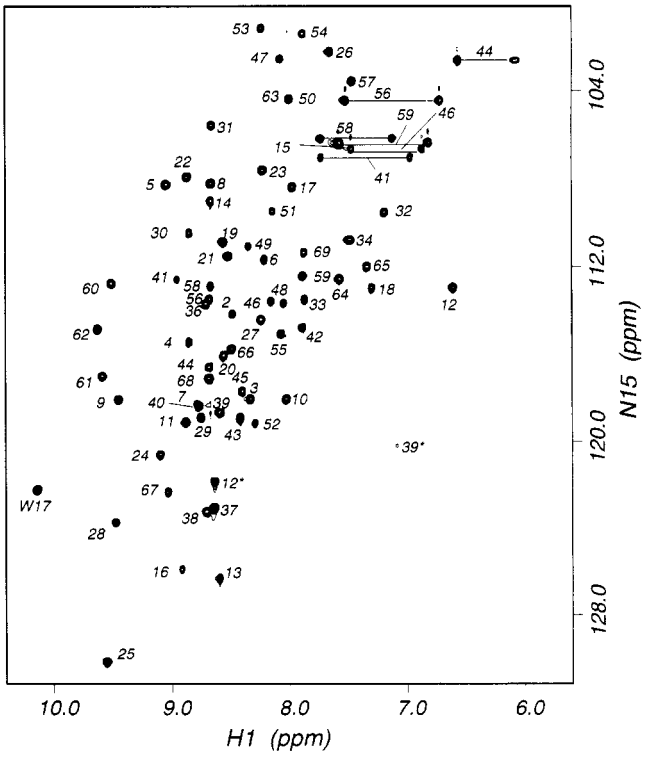

FIGURE 3: ^1H–^{15}N HSQC spectrum of PsaE with the assignments of the backbone ^{15}N amide protons. The $N^\epsilon H$ of Trp-17 is marked W17, and the Asn NH_2's are indicated by solid lines connecting their two proton resonances. Folded $N^\epsilon H$ resonances of two of the three Arg spin systems (12 and 39) are marked with an asterisk. The folded $N^\epsilon H$ of Arg-4 is detected at a lower contour level. This spectrum was collected under the same conditions as in Figure 1, with 32 transients for each of the 360 t_1 values.

displays a ^1H–^{15}N HSQC spectrum of PsaE at pH 5.8 with the sequentially determined ^1H–^{15}N assignments. The ^1H degeneracies are particularly obvious near 8.7 and 7.9 ppm, but it appears that these protons are coupled to ^{15}N nuclei with nondegenerate chemical shifts. The spectral overlap problems could therefore be alleviated with heteronuclear 3D experiments.

Figure 4 illustrates dipolar contacts in a composite presentation of five planes from the 3D ^{15}N NOESY-HSQC spectrum containing 9 of the 67 backbone amide resonances; both short- and long-range NOEs are observed from the

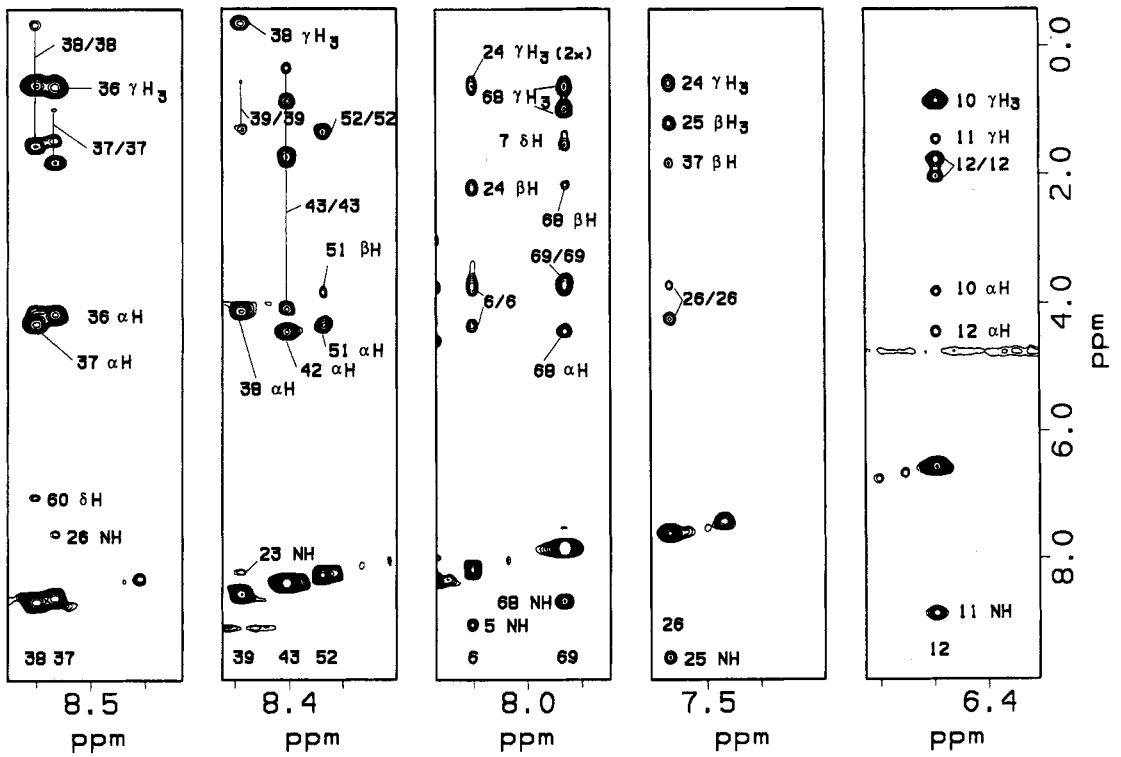

FIGURE 4: Composite of five planes taken from the 3D 120-ms ^{15}N NOESY–HSQC spectrum showing NOEs from residues 6, 12, 26, 37, 38, 39, 43, 52, and 69. Note the short-range NOEs [αN (i, i + 1) and NN(i, i + 1)] and several long-range NOEs for many of the amide resonances.

selected amide protons. The analysis of TOCSY and NOESY 3D data such as shown in Figure 4 yielded the remaining 30% assignments recalcitrant to 2D methods. Moreover, two Nα-(i, i) cross peaks (missing in both 2QF-COSY and TOCSY spectra because of saturation of the α proton along with the water resonance) were detected in a jump–return (Plateau & Guéron, 1982) NOESY spectrum (data not shown). The detection of these suppressed signals completes the sequential assignments, and all chemical shifts are listed in Table 1.

The stereospecific assignments and side-chain χ_1 angles were determined for residues containing a β-methylene group by using the following data: ^{15}N–H$_\beta$ J values obtained from the 2D H_NNH_{AB} COSY, the relative magnitude of NH–β2 and NH–β3 NOEs from the 3D ^{15}N NOESY–HSQC (or when resolved from the 70-ms ^{1}H NOESY), the relative magnitude of αH–β2/αH–β3 NOEs, and $J_{\alpha\beta}$ coupling information taken from the 3D ^{15}N TOCSY–HSQC or from the 2QF-COSY spectrum (Clore & Gronenborn, 1989). Stereospecific assignments and χ_1 angle determinations are not possible if C$^\beta$H$_2$'s are degenerate or if the pattern of NOEs suggests a conformationally averaged side chain. A thorough discussion of stereospecific assignments and χ_1 angle determination can be found elsewhere (Neri et al., 1992; Powers et al., 1993). Stereospecific assignments for the eight Val spin systems were made by using NH-to-C$^\gamma$H$_3$ and C$^\alpha$H-to-C$^\gamma$H$_3$ NOEs (Zuiderweg et al., 1985). Leucine stereospecific assignments of the C$^\delta$H$_3$ methyls were based on relative NOE intensities among NH, C$^\alpha$H, C$^\gamma$H, and C$^\delta$H$_3$ protons.

Regular Secondary Structure. Inspection of Figure 4 identifies sequential αN(i, i + 1) NOEs for amide (i + 1) protons 37, 38, 39, 52, and 69, and NN(i, i + 1) NOEs for amide (i) protons 5, 11, and 25. An extended conformation typical of a β-sheet is expected for the former group whereas a helical or turn conformation is likely for the latter. A full analysis of the 2D (as in Figure 2) and 3D (as in Figure 4) spectra reveals connectivities such as these for most of the backbone. Figure 5 summarizes the short-range and sequential NOEs for PsaE. Intense NOEs from αH of Tyr-34 to both δH$_2$'s of Pro-35 indicate a *trans* peptide configuration for the only Xxx–Pro bond. Also in Figure 5 are the results of correlated experiments carried out at pH 5.8 to identify slowly exchanging backbone amide hydrogens. Eighteen occurrences are indicated with a filled circle and are interpreted as H-bonded or buried hydrogens. Four amide signals, Ile-37, Val-38, Leu-65, and Glu-66, remain in the 2QF-COSY spectrum after 24 h of exchange, suggesting well-protected environments.

To characterize the secondary structure further, dihedral backbone angles ϕ were determined through the value of $^3J_{\alpha H\text{-}NH}$ coupling constants obtained in a series of J-modulated HSQC experiments (Neri et al., 1990). The cross-peak intensities were fit to eq 1 to extract the $^3J_{\alpha H\text{-}NH}$ values, and a Karplus relationship (De Marco et al., 1978) was applied to convert into a dihedral angle: coupling constants smaller than 6 Hz point to ϕ angles typical of turns (ca. −50°) whereas coupling constants larger than 8 Hz indicate extended structure (ca. −130°). Several intermediate values are obtained that are possibly due to conformational averaging. The J information is included in Figure 5.

The dominant motif of PsaE is extended structure. No substantial helical structure is anticipated as the few stretches of NN(i, i + 1) connectivities are adequately described by isolated turns causing chain reversal. Long-range NOEs reveal the global fold of the protein. For example, the C$^\alpha$H of Val-38 is in dipolar contact with the amide NH of Arg-39, and both of these protons are in dipolar contact with the C$^\alpha$H of Val-24. Thus, the peptide chain is extended between 38 and 39 and docks against position 24. Arg-39 has an NH-to-NH NOE to Thr-23, and Thr-23 shows a C$^\alpha$H-to-C$^\alpha$H NOE to Lys-7; this latter residue displays NOEs to the C-terminal Gly-69. From such information and the observed sequential NOEs, a β-sheet layout can be constructed. Figure 6 illustrates this, along with NOEs observed in 2D and 3D spectra (marked by dashed lines). The dipolar contacts are consistent with a

Table 1: ^{1}H and ^{15}N Chemical Shifts of PsaE[a]

	N	NH	αH	βH	others
A1			4.11	1.47	
I2	114.2	8.47	3.95	1.64	γ1H 0.93; 1.07; γ2H$_3$ 0.75; δH$_3$ 0.81
E3	118.1	8.33	4.54	2.02, 1.76[b]	γH 2.17
R4	115.5	8.85	3.61	1.65, 1.74	γH 1.40, 1.63; δH 3.24, 3.27; NεH 7.16; ^{15}Nε 78.1
G5	108.3	9.04	4.44, 3.41		
S6	111.6	8.20	4.37	3.78, 3.83	
K7	118.3	8.76	5.09	1.39, 1.60	γH 1.30; δH 1.46, 1.56; εH 2.85
V8	108.2	8.66	5.30	1.69	γH$_3$ 0.60, 0.48
K9	118.1	9.44	5.08	1.46, 1.66	γH 1.02, 1.07; δH 1.49, 1.49; εH 2.71
I10	118.1	8.02	3.85	2.60	γH 1.01, 1.79; γ2H$_3$ 0.91; δH$_3$ −0.11
L11	119.1	8.88	4.61	1.79, 1.54	γH 1.50; δH$_3$ 0.73, 0.81
R12	113.0	6.59	4.50	1.50, 1.84	γH 2.01, 2.10; δH 3.02, 3.45; NεH 8.62; ^{15}Nε 76.5
K13	126.3	8.59	2.87	1.42, 1.48	γH 0.98, 1.24; δH 1.43; εH 2.91
E14	109.1	8.66	4.14	2.03, 1.90	γH 2.16, 2.25
S15	106.5	7.55	4.41	3.93, 3.99	
Y16	125.9	8.92	3.96	1.49, 2.68	δH 5.65; εH 6.24
W17	108.4	7.97	4.30	2.99, 2.30	δH 6.80; ζ2H 7.50; ε3H 7.25; ζ3H 6.94; η2H 6.95; NεH 10.18; ^{15}Nε 122.2
Y18	113.0	7.29	3.88	2.63, 3.70	δH 6.86; εH 6.74
G19	110.9	8.55	3.80, 3.12		
D20	116.1	8.55	4.81	2.79, 2.79	
V21	111.5	8.50	5.14	1.85	γH$_3$ 0.76, 0.85
G22	107.9	8.86	4.51, 2.79		
T23	107.6	8.22	5.01	3.58	γ2H$_3$ 0.96
V24	120.6	9.09	3.75	2.28	γH$_3$ 0.62, 0.75
A25	130.2	9.56	4.33	1.25	
S26	102.2	7.64	4.31	3.76, 3.81	
I27	114.4	8.24	4.76	1.68	γ1H 1.02, 1.33; γ2H$_3$ 0.79; δH$_3$ 0.74
D28	123.8	9.47	4.60	2.56, 2.84	
K29	118.9	8.76	4.48	1.68, 2.11	γH 1.40, 1.52; δH 1.66, 1.70; εH 2.97
S30	110.5	8.85	4.31	3.90, 4.01	
G31	105.6	8.66	3.68, 4.19		
I32	109.6	7.18	4.29	2.01	γ1H 1.01, 1.51; γ2H$_3$ 0.82; δH$_3$ 0.80
I33	113.5	7.87	3.77	1.51	γ1H 0.91, 1.06; γ2H$_3$ 0.39; δH$_3$ 0.68
Y34	110.8	7.48	4.80	2.29, 2.83	δH 7.06; εH 6.79
P35			4.43	2.35, 2.25	γH 2.17, 2.01; δH 3.77, 3.88
V36	113.7	8.70	4.23	2.09	γH$_3$ 0.70, 0.83
I37	123.1	8.63	4.38	1.88	γ1H 1.03, 1.52; γ2H$_3$ 0.70; δH$_3$ 0.78
V38	123.2	8.70	4.19	1.63	γH$_3$ −0.27, 0.66
R39	118.7	8.58	4.79	1.41, 1.59	γH 1.43, 1.43; δH 3.08, 3.07; NεH 7.08; ^{15}Nε 78.2
F40	118.4	8.77	4.74	3.25, 2.34	δH 6.29; εH 6.38; ζH 6.57
N41	112.6	8.94	4.74	2.91, 2.82	NδH 6.98, 7.74; ^{15}Nδ 107.1
K42	114.8	7.89	4.51	1.96, 1.96	γH 1.37, 1.57; δH 1.60, 1.69; εH 2.75
V43	118.9	8.41	4.13	1.78	γH$_3$ 0.39, 0.92
N44	116.6	8.68	4.25	1.90, 2.71	NδH 6.08, 6.56; ^{15}Nδ 102.7
Y45	117.7	8.40	4.42	2.71, 3.15	δH 7.06; εH 6.75
N46	114.6	8.15	4.54	2.64, 2.71	NδH 6.86, 7.48; ^{15}Nδ 106.7
G47	102.6	8.07	3.73, 3.77		
F48	113.7	8.05	4.63	3.00, 3.14	δH 7.20; εH 7.32; ζH 7.27
S49	111.1	8.34	4.36	3.77, 3.82	
G50	104.4	7.99	3.85, 3.96		
S51	109.5	8.14	4.41	3.80, 3.88	
A52	119.2	8.29	4.38	1.41	
G53	101.1	8.23	3.92, 3.92		
G54	101.4	7.88	3.59, 3.69		
L55	115.1	8.07	4.68	1.72, 1.80	γH 1.75; δH$_3$ 1.02, 0.96
N56	113.5	8.68	5.15	3.41, 2.65	NδH 6.72, 7.52; ^{15}Nδ 104.5
T57	103.6	7.45	5.43	3.95	γ2H$_3$ 1.07
N58	112.9	8.66	4.80	2.62, 2.73	NδH 7.13, 7.74; ^{15}Nδ 106.2
N59	112.4	7.88	5.55	2.85, 2.47	NδH 6.82, 7.58; ^{15}Nδ 106.4
F60	112.8	9.51	4.47	3.35, 2.36	δH 7.05; εH 7.08; ζH 7.31
A61	117.0	9.58	5.03	1.57	
E62	114.9	9.63	3.70	2.11, 2.16	γH 2.30
H63	104.4	8.02	4.67	3.11, 3.44	δ2H 7.12; ε1H 8.00
E64	112.6	7.57	4.34	2.38, 2.54	γH 1.69, 1.97
L65	112.0	7.33	5.12	0.90, 1.85	γH 1.72; δH$_3$ 0.61, 0.34
E66	115.8	8.48	4.71	1.89, 1.96	γH 2.21, 2.21
V67	122.4	9.03	4.27	1.99	γH$_3$ 1.05, 0.96
V68	117.1	8.68	4.49	2.23	γH$_3$ 0.87, 0.69
G69	111.3	7.87	3.72, 3.83		

[a] Chemical shifts (±0.01 ppm) are reported at 298 K, pH 5.8, with respect to $^{1}H_2O$ at 4.76 ppm. [b] Underlined chemical shifts indicate stereospecific assignments for β-methylene groups (C$^{\beta 2}$H and C$^{\beta 3}$H, respectively), for valines (C$^{\gamma 1}$H$_3$ and C$^{\gamma 2}$H$_3$, respectively), and for leucines (C$^{\delta 1}$H$_3$ and C$^{\delta 2}$H$_3$, respectively). Three glycines could have their C$^{\alpha}$H$_2$'s stereospecifically assigned on the basis of the observed pattern of NOEs within the protein matrix and structure calculations. Reversing these assignments and those for isopropyl methyls resulted in large NOE violations (Falzone et al., 1994).

five-stranded antiparallel β-sheet with a (+1, +1, +1, −4x) topology equivalent to that observed in papain (Richardson, 1977). The strands are defined as follows: βA, 7–10; βB, 21–26; βC, 36–39; βD, 57–60; and βE, 65–68. Since the first

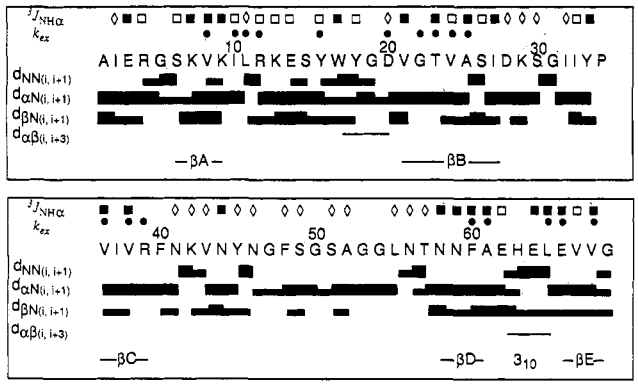

FIGURE 5: Summary of sequential information observed for PsaE at 298 K, pH 5.8. The top row contains $^3J_{\alpha H-NH}$ data: closed square symbols, $J > 8$ Hz; open square symbols, $J < 6$ Hz; diamonds, intermediate values. In the next row, dots mark the amide peaks remaining in the ^{15}N HSQC spectrum after PsaE was dissolved in ^2H_2O for 5 h at pH 5.8 (uncorrected for isotope effects). The bars below the sequence indicate the observed NOE connectivities: NN($i, i + 1$), $\alpha N(i, i + 1)$, $\beta N(i, i + 1)$, and $\alpha\beta(i, i + 3)$. Thicker bars denote larger intensity. Regular secondary structure is marked at the bottom. The single turn of 3_{10} helix (62–65) is consistent with the observed NOE and amide hydrogen-exchange patterns. The $\alpha N(i, i + 1)$ connectivity between Phe-40 and Asn-41 is tentative because of the overlap of the α protons for these residues.

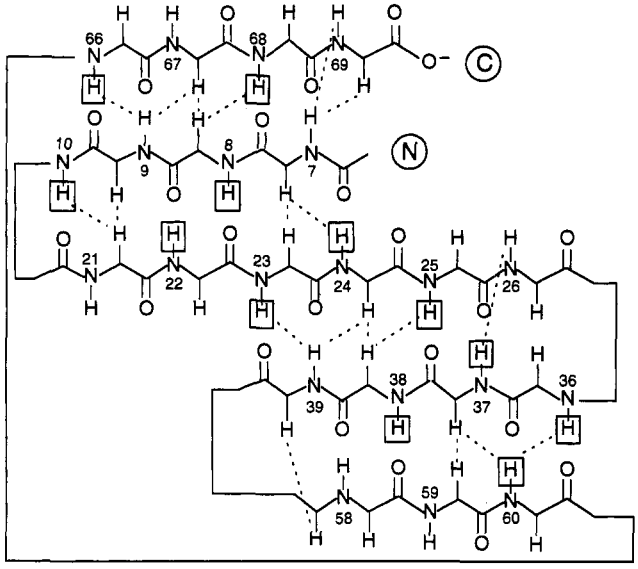

FIGURE 6: Layout of the five-stranded β-sheet found in PsaE. The observed NOEs are indicated by dotted lines, and the slowly exchanging amide protons are boxed. Note that the middle strand, βB, spans residues 21–26 and is in contact with strands βA (7–10) and βC (36–39). These two strands overlap by only two residues on βB.

and third strands dock on the second by sharing only two residues, an alternative representation uses two three-stranded β-sheets. As commonly observed in globular proteins, the C-terminus of the protein is close to its N-terminus.

Loops and Turns. Long-range NOEs are observed past strand βC for residues 40 through 45, but no regular secondary structure is expected in this segment, which lacks the typical dipolar contacts. A particular feature of the next eight residues (46–53) is the absence of long-range NOEs. These are again observed for Gly-54 whose $C^\alpha H$'s are in weak dipolar contact with the ring of Tyr-45. A weak NOE between one of the α protons of Gly-54 and one of the $C^\gamma H_3$'s of Val-43 is also observed. The scarcity of NOEs constraining the loop spanning residues 42–56 suggests a disordered conformation between the third (βC) and fourth (βD) strands. Other segments not adopting regular extended structure include residues 1–5, 11–19, 27–34, and 61–65. Among these, stretches 16–19 and 62–65 show NN($i, i + 1$) NOEs over a four-residue span indicating a well-defined turn. Residues 16–19 display NOEs characteristic of a type I turn, and Glu-62 and Leu-65 have an $\alpha\beta(i, i + 3)$ contact suggesting a 3_{10} helical conformation or a type III turn. This is consistent with the slow amide exchange of Leu-65 (i) which would form a hydrogen bond to the carbonyl of Glu-62 ($i - 3$). No $\alpha N(i, i + 3)$ interactions are detected.

Hydrophobic Cluster. The assignment process was facilitated by the NOEs among a set of residues participating in a hydrophobic cluster. The central residue of this cluster is Phe-40, a conserved amino acid across known PsaE proteins (Zhao et al., 1993). Phe-40 is surrounded by several nonpolar side chains including Val-8, Ile-10, Trp-17, Val-38, and Phe-60. These side chains are appended to strand βA and the loop between βA and strands βB, βC, and βD. Phe-40 also shows NOEs to Gly-22 in the βB strand. Phe-60 has NOEs to Ile-10, Val-36, Val-38, Phe-40, and Leu-65. The unique stretch Tyr-Trp-Tyr (16–18) in the AB segment of the protein defines the boundary of the core. Tyr-16 contacts Trp-17, which in turn has weak NOEs to Val-43 and Leu-55 and, as mentioned above, Phe-40. Tyr-18 has NOEs to Leu-11 and Leu-11 to Leu-65, thus completing the hydrophobic contacts in the interior of the protein. The cluster contains a number of conserved residues other than Phe-40: Val-8, Ile-10, Tyr-16, Trp-17, Val-36, and Val-38 are all present in variants of PsaE (Zhao et al., 1993). They ensure tight packing in the core of the protein and constitute an important feature of the solution structure.

$pK_{1/2}$ of His-63. When PS I complexes are isolated from *Synechococcus* sp. strain 7002 at pH 8.0, the PsaE subunit is found associated with the PS I trimers. However, at pH 9.0 or at pH values below 7.0, the PS I trimers do not contain the PsaE subunit. For example, incubation of the PS I complexes at pH 7.0 at room temperature for 45 min led to the complete extraction of PsaE from the complex. This behavior suggested that pH might affect the conformation of the PsaE protein (or one of its interaction partners) in some manner to cause release of the protein from the complex. PsaE contains a single histidine (residue 63) that is located in the last turn between the βD and βE strands, and in view of the results described above, preliminary pH dependence studies to determine the involvement of His-63 in possible conformational regulation were performed. The pH response of the chemical shift of the $C^\epsilon H$ and $C^\delta H$ of the imidazole group is plotted in Figure 7. The continuous line is the result of a fit to the Henderson–Hasselbalch equation. The $pK_{1/2}$ of the histidine is 5.35 (±0.01, standard deviation of the fit) and the Hill coefficient 0.84 (±0.02, standard deviation of the fit). The $pK_{1/2}$ value indicates that, at physiological pH and below pH 7 where incubation causes the loss of PsaE, the imidazole group is in the neutral form. Unless interactions with other proteins or the membrane raise the $pK_{1/2}$, His-63 does not appear to be involved in this particular regulation.

Native protein signals have full intensity down to pH 4. Below that value, a second set of resonances appears in the spectrum. This second set, from acid-unfolded protein, grows in intensity at the expense of the native set as the pH is lowered. The inset in Figure 7 represents the apparent fraction of native form as determined by relative integrated peak intensity versus pH. The solid line is the result of a two-state fit. The midpoint of the transition occurs at pH 2.9. The chemical shift separation between the lines of the two forms shows that the exchange between native and acid-unfolded conformations takes place slowly on the NMR time scale, at a rate lower than 50 s^{-1} at 298 K.

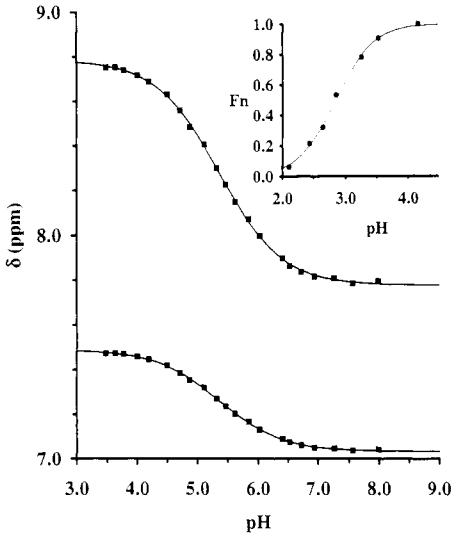

FIGURE 7: Response of the single histidine residue to pH variation. The chemical shift of the C^{δ} and C^{ϵ} protons is plotted versus pH in the lower and upper curves, respectively. The solid line is the result of a nonlinear least-squares fit to the Henderson–Hasselbalch equation. The apparent $pK_{1/2}$ is 5.35. The inset contains a plot of the apparent fraction of native conformation at site 63 versus pH. The apparent fraction was obtained by comparing the integrated intensity of the native and acid-unfolded $C^{\epsilon}H$ signal in the simulated 1D spectrum. The solid line represents the fit to a two-state model (Henderson–Hasselbalch equation). The midpoint of the transition occurs at pH 2.9.

In conclusion, the topology of PsaE was determined with NOE information, $^3J_{\alpha H-NH}$ values, and hydrogen-exchange data. The major structural feature of this protein is a five-stranded β-sheet with all strands antiparallel. A large loop spanning residues 42–56 with no long-range constraints for the segment stretching from Asn-46 to Gly-53 is also a unique feature of the three-dimensional solution structure. The global fold revealed by the NMR experiments explains the absence of detected electron density corresponding to this small protein in the recent X-ray structure of PS I (Krauss et al., 1993). The three-dimensional structure of the protein in solution is presented in the companion paper.

ACKNOWLEDGMENT

D. A. Bryant thanks Dr. John H. Golbeck for helpful discussions. Dr. Alan J. Benesi and John G. Lintner of the NMR facility are gratefully acknowledged for their participation in the spectrometer modification.

REFERENCES

Andersen, B., Scheller, H. V., & Møller, B. L. (1992) *FEBS Lett. 311*, 169–173.

Bax, A., Ikura, M., Kay, L. E., & Zhu, G. (1991) *J. Magn. Reson. 91*, 174–178.

Billeter, M., Neri, D., Otting, G., Qian, Y. Q., & Wüthrich, K. (1992) *J. Biomol. NMR 2*, 257–274.

Bodenhausen, G., & Ruben, D. G. (1980) *Chem. Phys. Lett. 69*, 185–189.

Bodenhausen, G., Kogler, H., & Ernst, R. R. (1984) *J. Magn. Reson. 58*, 370–388.

Böttcher, B., Gräber, P., & Boekema, E. J. (1992) *Biochim. Biophys. Acta 1100*, 125–136.

Braunschweiler, L., & Ernst, R. R. (1983) *J. Magn. Reson. 53*, 521–528.

Braunschweiler, L., Bodenhausen, G., & Ernst, R. R. (1983) *Mol. Phys. 48*, 535–560.

Bryant, D. A. (1992) in *The Photosystems: Structure, Function and Molecular Biology* (Barber, J., Ed.) Vol. 11, pp 501–549, Elsevier, Amsterdam.

Bryant, D. A., Rhiel, E., de Lorimier, R., Zhou, J., Stirewalt, V. L., Gasparich, G. E., Dubbs, J. M., & Snyder, W. (1990) in *Current Research in Photosynthesis* (Baltscheffsky, M., Ed.) Vol. II, pp 1–9, Kluwer, Dordrecht.

Bundi, A., & Wüthrich, K. (1979) *Biopolymers 18*, 285–297.

Chary, K. V. R., Otting, G., & Wüthrich, K. (1991) *J. Magn. Reson. 93*, 218–224.

Chitnis, P. R., & Nelson, N. (1991) in *Cell Culture and Somatic Cell Genetics of Plants* (Bogorad, L., & Vasil, I. K., Eds.) Vol. 7B, pp 177–224, Academic Press, New York.

Chitnis, P. R., Reilly, P. A., Miedel, M. C., & Nelson, N. (1989) *J. Biol. Chem. 264*, 18374–18380.

Clore, G. M., & Gronenborn, A. M. (1989) *Crit. Rev. Biochem. Mol. Biol. 24*, 479–564.

De Marco, A., Llinás, M., & Wüthrich, K. (1978) *Biopolymers 17*, 637–650.

Drobny, G., Pines, A., Sinton, S., Weitekamp, D. P., & Wemmer, D. (1979) *Symp. Faraday Soc. 13*, 49–55.

Falzone, C. J., Kao, Y.-H., Zhao, J., Bryant, D. A., & Lecomte, J. T. J. (1994) *Biochemistry* (following paper in this issue).

Golbeck, J. H. (1992) *Annu. Rev. Plant Physiol. Plant Mol. Biol. 43*, 293–324.

Golbeck, J. H. (1994) in *The Molecular Biology of Cyanobacteria* (Bryant, D. A., Ed.) Kluwer, Dordrecht (in press).

Golbeck, J. H., & Bryant, D. A. (1991) in *Light Driven Reactions in Bioenergetics* (Lee, C. P., Ed.) Vol. 16, pp 83–177, Academic Press, New York.

Kay, L. E., Ikura, M., Tschudin, R., & Bax, A. (1990) *J. Magn. Reson. 89*, 496–514.

Krauss, N., Hinrichs, W., Witt, I., Fromme, P., Pritzkow, W., Dauter, Z., Betzel, C., Wilson, K. S., Witt, H. T., & Saenger, W. (1993) *Nature 361*, 326–331.

Kruip, J., Boekema, E. J., Bald, D., Boonstra, A. F., & Rögner, M. (1993) *J. Biol. Chem. 268*, 23353–23360.

Kumar, A., Ernst, R. R., & Wüthrich, K. (1980) *Biochem. Biophys. Res. Commun. 95*, 1–6.

Li, N., Warren, P. V., Golbeck, J. H., Frank, G., Zuber, H., & Bryant, D. A. (1991a) *Biochim. Biophys. Acta 1059*, 215–225.

Li, N., Zhao, J. D., Warren, P. V., Warden, J. T., Bryant, D. A., & Golbeck, J. H. (1991b) *Biochemistry 30*, 7863–7872.

Maniatis, T., Fritsch, E. F., & Sambrook, J. (1982) *Molecular Cloning: A Laboratory Manual*, Cold Spring Harbor Press, Cold Spring Harbor, NY.

Marion, D., & Wüthrich, K. (1983) *Biochem. Biophys. Res. Commun. 113*, 967–974.

Marion, D., Ikura, M., Tschudin, R., & Bax, A. (1989) *J. Magn. Reson. 85*, 393–399.

Neri, D., Otting, G., & Wüthrich, K. (1990) *J. Am. Chem. Soc. 112*, 3663–3665.

Neri, D., Billeter, M., & Wüthrich, K. (1992) *J. Mol. Biol. 223*, 743–767.

Otting, G., Widmer, H., Wagner, G., & Wüthrich, K. (1986) *J. Magn. Reson. 66*, 187–193.

Parrett, K. P., Mehari, T., & Golbeck, J. H. (1990) *Biochim. Biophys. Acta 1015*, 341–352.

Plateau, P., & Guéron, M. (1982) *J. Am. Chem. Soc. 104*, 7310–7311.

Powers, R., Garrett, D. S., March, C. J., Frieden, E. A., Gronenborn, A. M., & Clore, G. M. (1993) *Biochemistry 32*, 6744–6762.

Rance, M. (1987) *J. Magn. Reson. 74*, 557–564.

Rance, M., & Byrd, R. A. (1983) *J. Magn. Reson. 54*, 221–240.

Rance, M., & Wright, P. E. (1986) *J. Magn. Reson. 66*, 372–378.

Rance, M., Sørensen, O. W., Bodenhausen, G., Wagner, G., Ernst, R. R., & Wüthrich, K. (1983) *Biochem. Biophys. Res. Commun. 117*, 479–485.

Richardson, J. S. (1977) *Nature 268*, 495–500.

Rousseau, F., Sétif, P., & Lagoutte, B. (1993) *EMBO J. 12*, 1755–1765.

Schluchter, W. M., & Bryant, D. A. (1992) *Biochemistry 31*, 3092–3102.
Shaka, A. J., Keeler, J., & Freeman, R. (1983) *J. Magn. Reson. 53*, 313–340.
Shaka, A. J., Barker, P. B., & Freeman, R. (1985) *J. Magn. Reson. 64*, 547–552.
Shaka, A. J., Lee, C., & Pines, A. (1988) *J. Magn. Reson. 77*, 274–293.
Sonoike, K., Hatanaka, H., & Katoh, S. (1993) *Biochim. Biophys. Acta 1141*, 52–57.
Stevens, S. E. J., Patterson, C. O. P., & Myers, J. (1973) *J. Phycol. 9*, 427–430.
Weber, N., & Strotmann, H. (1993) *Biochim. Biophys. Acta 1143*, 204–210.
Wüthrich, K. (1986) *NMR of Proteins and Nucleic Acids*, Wiley, New York.
Yu, L., Zhao, J., Mühlenhoff, U., Bryant, D. A., & Golbeck, J. H. (1993) *Plant Physiol. 103*, 171–180.
Zhao, J., Snyder, W. B., Mühlenhoff, U., Rhiel, E., Warren, P. V., Golbeck, J. H., & Bryant, D. A. (1993) *Mol. Microbiol. 9*, 183–194.
Zuiderweg, E. R. P., Boelens, R., & Kaptein, R. (1985) *Biopolymers 24*, 601–611.